Molecular Analysis of Apoptotic and Stress-Related Genes in Rotenone-induced Parkinson's Disease Model using SH-SY5Y cells

Gomathi R[1], Rohini D[1*]

[1]Department of Biochemistry, School of Life Sciences, Vels Institute of Science, Technology & Advanced Studies

[*]Corresponding author e-mail: drrohinidurairaj@gmail.com

ABSTRACT

Objectives: Parkinson's disease (PD) is a progressive neurodegenerative disorder characterized by dopaminergic neuronal degeneration, oxidative stress, mitochondrial dysfunction, and apoptosis. The present study aimed to evaluate the neuroprotective efficacy of Tridax procumbens leaf extract (TPL) and its green synthesized silver nanoparticles (TPL-AgNPs) against rotenone-induced neurotoxicity in SH-SY5Y human neuroblastoma cells, using levodopa (LDA) as a standard reference drug. Silver nanoparticles were synthesized via an eco-friendly method and characterized by UV–Vis spectroscopy, FTIR, SEM, TEM, EDX, and XRD analyses.

Methods: An in-vitro model was established by exposing SH-SY5Y cells to rotenone. Cell viability and cytotoxicity were assessed using the MTT assay. Intracellular reactive oxygen species (ROS) production and mitochondrial membrane potential (ΔΨm) loss were evaluated by DCFH-DA and Rhodamine 123 fluorescent staining, respectively. Nuclear apoptotic changes were examined using PI, DAPI, and AO/EB staining. The mRNA expression levels of apoptotic markers (Bax, Bcl-2, caspase-3) and endoplasmic reticulum stress related signalling molecule ERK1 were quantified by RT-qPCR analysis.

Results: Rotenone exposure significantly reduced cell viability, elevated ROS generation, disrupted mitochondrial membrane potential, increased ERK1 expression, upregulated pro-apoptotic genes (Bax and caspase-3), and downregulated anti-apoptotic Bcl-2 expression. Pretreatment with TPL, TPL-AgNPs, and LDA significantly attenuated oxidative stress, restored mitochondrial function, reduced nuclear apoptosis, and modulated apoptotic and ERK1 gene expression in a dose-dependent manner. Notably, TPL-AgNPs exhibited enhanced neuroprotective activity compared to the crude extract and showed comparable protective effects to LDA.

Conclusion: The green synthesized TPL-AgNPs exert significant neuroprotective effects against rotenone-induced oxidative stress, mitochondrial dysfunction, stress related signalling molecule, and apoptosis in SH-SY5Y cells, highlighting their potential as a promising therapeutic strategy for neuroprotective management.

Keywords: Tridax procumbens Linn, Ag-nanoparticles, MTT, ROS, DCFH-DA, PI, DAPI and AO/EB staining

How to cite this article: Gomathi R, Rohini D. Molecular Analysis of Apoptotic and Stress-Related Genes in Rotenone-induced Parkinson's Disease Model using SH-SY5Y cells. Int J Drug Deliv Technol. 2026;16(5): 1301-1312. DOI: 10.25258/ijddt.16.5.120

Source of support: Nil.

Conflict of interest: None

Introduction

One of the most complicated and delicate phases of human development is neurodevelopment, which takes place from childhood until puberty. Even little disruptions of the neurodevelopmental pathways can produce major diseases like dementia and autism spectrum disorder since the brain is still developing and sensitive [1]. Neuronal dysfunction is recognized to be primarily caused by a number of genetic-related variables. Many of the environmental factors that humans are frequently exposed to have the potential to be harmful. Nanoparticles with at least one dimension less than 100 nm have gained attention recently [2]. Because they frequently have better physicochemical qualities than traditional materials, nanoparticles can be used in a wide range of industries, such as food, medicine, and cosmetics. For instance, due of their strong antibacterial properties, silver nanoparticles are now found in common place items including clothing, masks, dining utensils, and antibacterial sprays. In that, the breast milk can allow silver nanoparticles to enter the developing mouse brain through blood brain barrier Therefore, in order to ensure the safe use of silver nanoparticles, a more thorough understanding of their impacts on neurodevelopment is essential. Native to Central and South America, *Tridax*

procumbens, sometimes referred to as "coat buttons," is an annual plant belonging to the Asteraceae family [3]. Alkaloids, flavonoids, tannins, and terpenoids are among the many bioactive substances found in the highly promising species *Tridax procumbens* [4]. These compounds exhibit immunomodulatory, anti-oxidant, anti-hepatotoxic, analgesic, antidiabetic, anti-inflammatory, antifungal, neuroprotective, and antimicrobial properties. Parkinson's disease is characterized by dopaminergic (DA) neuron degeneration in the substantia nigra pars compacta, accompanied with locomotors defects and its slowly developing neurological condition that impairs motor function and results in tremor, sluggish movements, and abnormalities in gait and balance. It is the second most common neurodegenerative disease worldwide with incidence and prevalence on the rise along with changing population demographics [5,6]. The neurotoxic animal models of Parkinson's disease (PD) reflect some important neurobehavioral or pathological characteristics, despite the fact that the pathology of PD is poorly understood. The neurotoxins can cause parkinsonism both *in-vitro* and *in-vivo*, such as 6-hydroxydopamine, 1-methyl-4-phenyl-1,2,3,6-tetrahydropyridine, paraquat, and rotenone [7,8,9]. Rotenone (R), a lipophilic pesticide, can cross cell membrane easily to induce systemic inhibition of mitochondrial complex I and cause selective nigrostriatal dopaminergic degeneration. Rotenone-induced apoptosis in human neuroblastoma SH-SY5Y cells was mediated by the generation of mitochondrial reactive oxygen species (ROS) and rhodamine 123 [10]. Apoptosis regulator is B-cell lymphoma- 2 (Bcl-2) family of proteins, which have a crucial role in intracellular apoptotic signalling and which include both pro- and anti-apoptotic proteins. The major members of this family are Bcl-2, Bcl-xL and Bax. Bcl-2 and Bcl-xL are localized to the mitochondrial outer membrane, to the endoplasmic reticulum and perinuclear membrane [11]. Therefore, this study aims to investigate the neuroprotective effects of TPL and TPL-AgNPs on rotenone-induced cellular toxicities (SH-SY5Y cells) *in-vitro*.

Materials and Methods

TPL, TPL-AgNPs, Rotenone, retinoic acid, Dulbecco's modified Eagle's medium (DMEM), Fetal bovine serum solution, Dimethyl sulfoxide, 5-diphenyl-tetrazolium bromide (MTT), dichlorofluorescein diacetate (DCFH-DA), rhodamine 123, 4',6-diamidino-2-phenylindole (DAPI), dimethyl sulphoxide (DMSO), Trypsin–EDTA solution, 3-(4,5-Dimethylthiazol-2-yl)-2,5-Diphenyltetrazolium, 70% ethanol, propidium iodide.

Collection of sample and preparation of leaf extract

In Tamil Nadu, India's Chengalpattu district, the plant was gathered locally. It was verified by the University of Madras' Botany Department in Guindy. After being removed from the plant, the leaves were thoroughly cleaned with water. The cleaned leaves were then allowed to dry completely in the shade before being ground into a fine powder in a mechanical grinder and kept in airtight containers. Then, 10 grams of powder were extracted. Cold extraction was carried out using the maceration method with hydro-ethanol (ethanol&water-70:30) for 24 hours using the "intermittent shaking" method to obtain extracts. Whatman filter no. 1 paper was used to filter for further analysis [12].

Synthesis and characterisation of TPL-AgNps

In the biosynthesis of AgNPs, this approach involved filling a 250 ml flask with 45 ml of 1 mM aqueous AgNO3 solution and adding 5 ml of leaf extract. After that, the flask was left at room temperature for five hours in the dark to reduce the amount of silver nitrate photoactivation. Additionally, a control setup was maintained without extract. The resulting TPL-AgNPs solution was purified by repeatedly centrifuging it for 15 minutes at 10,000 rpm and then re-dispersing the pellet in de-ionized water. The synthesis of TPL-AgNps was ascertained by colour change from yellow to green [13]. The characterisation of TPL-AgNPs shows UV-Visible spectroscopy revealed the absorption was observed at 439.20nm. The average size of obtained TPLAgNPs particle was found to be 76.24 ± 13.19 nm with polydispersed and spherical in shape. Antioxidant activity was tested against DPPH assay reveals that IC50 value of 52.66 μg/mL. The antioxidant activity of TPL-AgNPs showed 92% inhibition at the concentration of 100 μg/mL [14,15].

Cell culture

The SH-SY5Y cells were obtained from the National Centre for Cell Science (NCCS), Pune, India. SH-SY5Y cells were cultured in DMEM supplemented with 10% FBS and 1% antibiotics, maintained at 37°C with 5% CO_2. Cells were differentiated using 10 µM retinoic acid for 7 days [16]. Rotenone (20 µM) was used to induce toxicity for 24 h [17,18,19]. TPL and TPL-AgNPs were prepared in DMSO (<0.1%) and evaluated for their neuroprotective effects against rotenone-induced damage.

Cell viability assay

Cell viability of TPL, TPL-AgNPs, and rotenone was assessed in SH-SY5Y cells cultured in DMEM with 10% FBS and 1% antibiotics at 37 °C, 5% CO_2. Cells were seeded at 5000 cells/well and treated with varying concentrations (0, 10, 20, 40, 80, 150 and 250 µM) for 24 h. MTT assay (1 mg/mL, 3 h) was performed, and absorbance was measured at 450 nm. Results were expressed as % viability relative to control. Experiments were conducted in triplicate, and the effective doses were selected for further analysis [20].

Reactive oxygen species (ROS) & mitochondrial membrane potential

Intracellular ROS levels were measured using DCFH-DA assay. SH-SY5Y cells (8×10^4 cells/well) were cultured and treated with rotenone (20 µM) for 24 h, followed by TPL, TPL-AgNPs, and LDA at EC_{50} concentrations for another 24 h. Cells were then incubated with DCFH-DA (10 µM) for 30 min in the dark, washed with PBS, and fluorescence was observed using an inverted fluorescence microscope [21,22]. Mitochondrial membrane potential ($\Delta\Psi m$) was assessed using Rhodamine 123 staining. SH-SY5Y cells (2×10^4 cells/well) were treated with rotenone (20 µM) for 24 h, followed by TPL, TPL-AgNPs, and LDA for another 24 h. Cells were then incubated with R-123 (10 µg/mL) for 20–30 min in the dark, washed with PBS, and fluorescence images were captured using an inverted fluorescence microscope.

Cellular morphology and nuclear apoptosis

PI Staining: After treatment, cells were harvested, washed with PBS, and fixed in 70% ethanol at −20°C for ≥2 h. Following centrifugation, cells were resuspended in PBS and stained with propidium iodide (5 µg/mL) for 30 min in the dark. Nuclear morphology was then observed using a fluorescence microscope [23].

DAPI Staining: Cells were resuspended in PBS and stained with DAPI (1 µg/mL) for 30 min at room temperature in the dark. Nuclear morphology was then observed and imaged using a fluorescence microscope. [24].

Dual staining: Cell and nuclear morphology were assessed using AO/EB staining. Cells were trypsinized, ethanol-fixed, and stained with AO/EB dye mixture (1:1). Stained cells were immediately observed under an inverted fluorescence microscope to identify apoptotic changes. [25].

RNA isolation

Total RNA was extracted from SH-SY5Y cells using TRIzol reagent following standard protocol. Cells treated with rotenone (20 µM) were lysed, phase-separated with chloroform, and RNA was precipitated using isopropanol. The RNA pellet was washed with 75% ethanol, air-dried, and resuspended in RNase-free water. RNA quality and quantity were assessed using Nanodrop and agarose gel electrophoresis, and samples were stored at −80°C for further use. [26].

qPCR analysis

qPCR was performed using cDNA (10–50 ng), gene-specific primers (Bax, BCL2, Caspase-3, ERK1), and SYBR Green master mix. Reactions (10–20 µL) were run with initial denaturation at 95°C, followed by 35–40 cycles of denaturation, annealing (55–60°C), and extension. Gene expression was normalized to β-actin, and relative expression was calculated using the $2^{-}\Delta\Delta Ct$ method.

Result and discussion:

In this study, we evaluated the effects of TPL and TPL-AgNPs with standard LDA on rotenone-induced cell death, nuclear apoptosis, production of intracellular ROS, loss of ΔΨm, expressions of Bax, Bcl-2, caspase-3 and phosphorylation of ERK1s in SH-SY5Y cells.

Cell viability assay

The cytoprotective effect of TPL, TPL-AgNPs, and standard LDA against rotenone-induced toxicity was evaluated using the MTT assay, which measures mitochondrial activity by converting MTT into formazan crystals shown in **figure 1**. Rotenone treatment significantly reduced cell viability ($P < 0.01$) in SH-SY5Y cells, with an IC_{50} value of 20 µM. After rotenone exposure, cells were treated with different concentrations of TPL and TPL-AgNPs for 24 hours shown in **figure 2a & 2b**. The IC_{50} values were 138.45 µg/ml for TPL and 45.85 µg/ml for TPL-AgNPs.

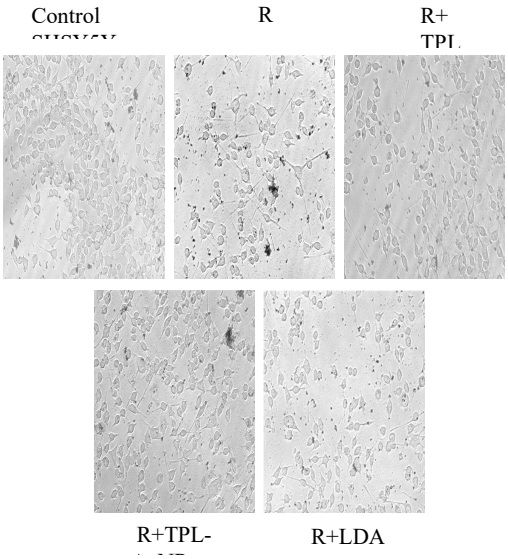

Figure: 1 The morphological change was visualized by phase-contrast imaging. Scale bar: 50 µm.

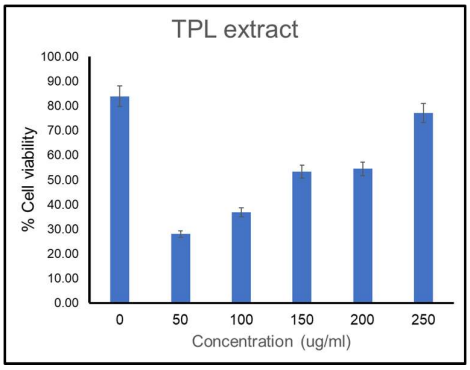

Figure:2a

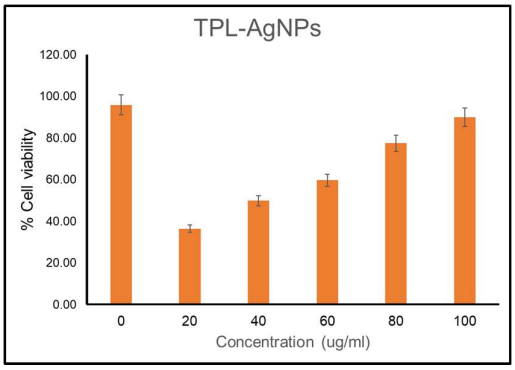

Figure:2b

Figure:2a & 2b Illustrate the percentage of cell viability of TPL and TPL-AgNPs at different concentration on rotenone-induced cell death in SH-SY5Y differentiated human cell line.

Determination of intracellular reactive oxygen species (ROS) & Changes in mitochondrial membrane potential

The protective effect of TPL & TPL-AgNPs against rotenone-induced ROS generation was assessed using the DCFH-DA fluorescent probe. Rotenone-treated cells showed a significant increase in ROS levels compared to control cells, while TPL and TPL-AgNPs reduced ROS, indicating their antioxidant activity shown in **figure 3a&3b** [28,29]. Rotenone inhibits mitochondrial complex I, leading to loss of mitochondrial membrane potential (ΔΨm) and release of pro-apoptotic proteins [30]. This was confirmed by a two-fold decrease in Rh123 fluorescence after rotenone treatment ($P < 0.05$) shown in **figure 4a&4b**. However, treatment with TPL and TPL-AgNPs for 6 hours did not significantly affect ΔΨm compared to the control, suggesting their protective role [31].

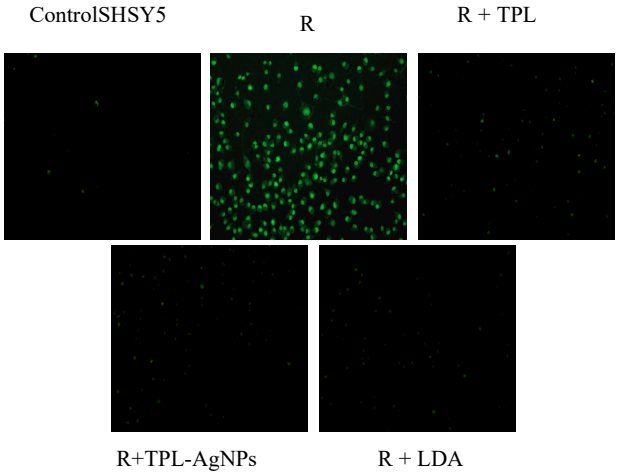

Figure:3a

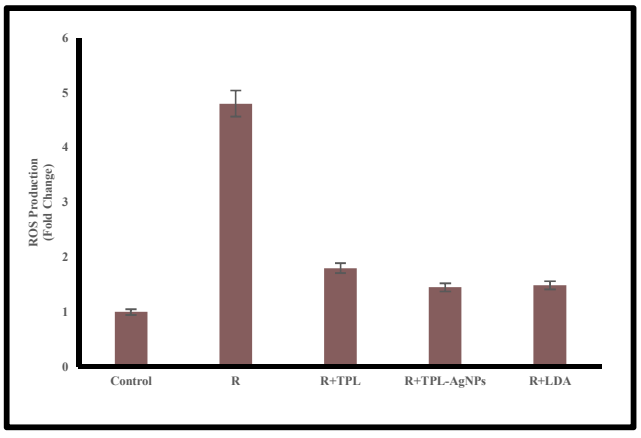

Figure:3b

Figure 3a & 3b: (A) Illustrate the ROS generation was determined by the mean fluorescent intensity (MFI) of DCFH-DA representative fluorescent images. Scale bar: 50 µm. (B) Statistical analysis. At least 600 randomly selected cells were counted in each experiment (n = 3, #$P < 0.05$ versus control, *$P < 0.05$ versus treated samples).

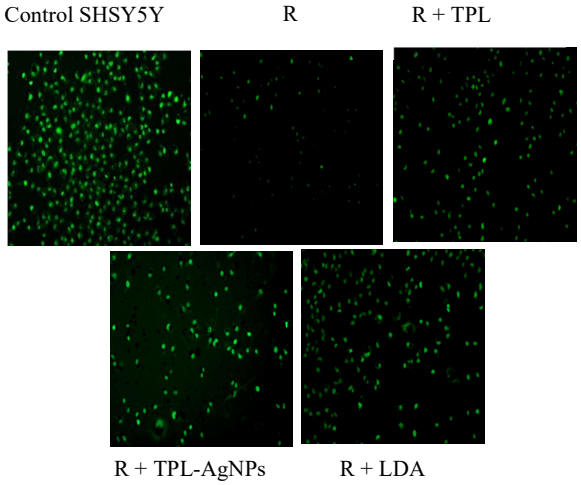

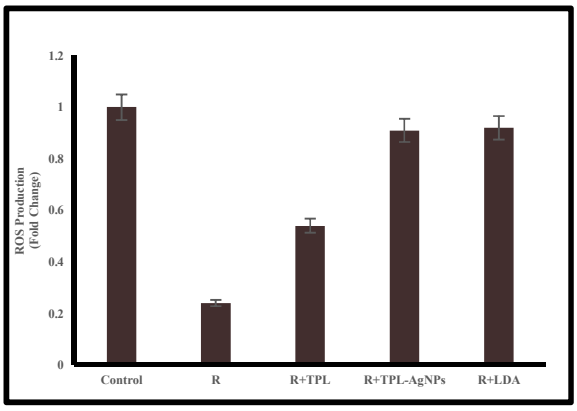

Figure:4a

Figure:4b

Figure 4a & 4b: (A) Illustrate the ΔΨm was determined by the mean fluorescent intensity (MFI) of Rh123, representative fluorescent images. Scale bar: 50 µm. (B) Statistical analysis. At least 600 randomly selected cells were counted in each experiment (n = 3, #P < 0.05 versus control, *P < 0.05 versus treated samples).

Cellular morphology and nuclear apoptosis

PI staining: PI staining was used to assess cell viability and cell cycle by flow cytometry. Since PI stains only dead cells by binding to DNA, increased red fluorescence indicates higher cell death. Flow cytometry results showed a higher percentage of PI-positive cells in rotenone-treated SH-SY5Y cells compared to control, R+TPL, R+TPL-AgNPs, and R+LDA groups, indicating increased cell death with rotenone treatment [32] **figure 5a & 5b**.

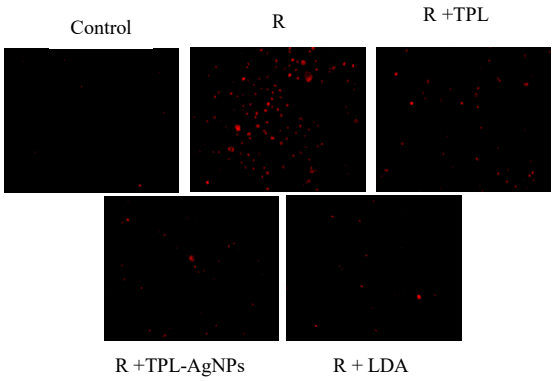

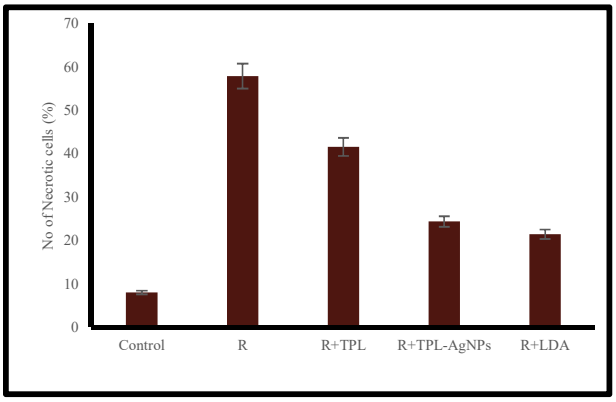

Figure:5a

Figure:5b

Figure 5a & 5b: (A) ISllustrate the PI staining was performed to evaluate cell death in treated samples, representative fluorescence images of PI-stained cells under different conditions: Control, rotenone, R+TPL, R+TPL-AgNPs and R+LDA. Red fluorescence indicates PI-positive (dead/apoptotic) cells. Scale bar: 50 µm. (B) Quantification of PI-positive cells

expressed as a percentage of total cells. The differentiated human SH-SY5Y cell line treated with rotenone significantly increased cell death, whereas other treated samples reduced PI staining, indicating its neuroprotective effect. Statistical analysis. At least 600 randomly selected cells were counted in each experiment (n = 3, #P < 0.05 versus control, *P < 0.05 versus treated samples).

DAPI staining: DAPI staining was used to observe nuclear changes related to apoptosis. Normal cells showed round and uniformly stained nuclei, while apoptotic cells exhibited nuclear condensation and fragmentation. Rotenone-treated SH-SY5Y cells showed more fragmented and shrunken nuclei compared to control, R+TPL, R+TPL-AgNPs, and R+LDA groups, confirming increased apoptosis [33] **figure 6a&b.**

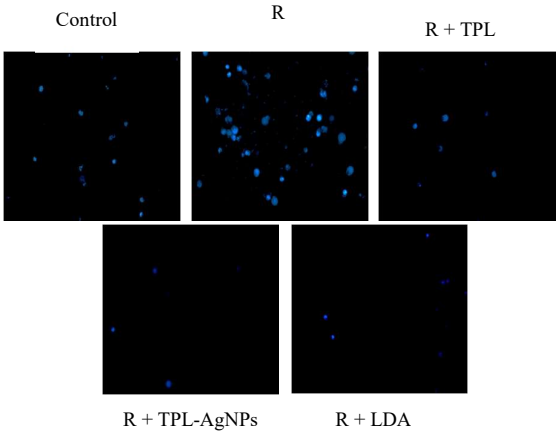

Figure:6a

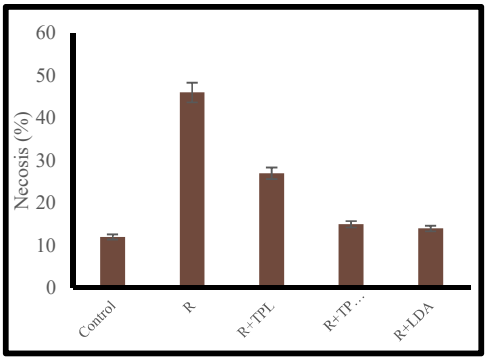

Figure:6b

Figure 6a&b: (A) Illustrate the DAPI staining was performed to evaluate nuclear integrity and apoptosis in treated samples, representative fluorescence images of DAPI-stained nuclei under different conditions: Control, rotenone, R+TPL, R+TPL-AgNPs and R+LDA. Intact nuclei appear as uniform blue fluorescence, while fragmented or condensed nuclei indicate apoptotic cells. Scale bar: 50 μm. (B) Quantification of apoptotic nuclei (% of total nuclei) shows a significant increase in nuclear fragmentation in the differentiated human SH-SY5Y cell line treated with rotenone, while Control, R+TPL, R+TPL-AgNPs and R+LDA reduced apoptotic changes, suggesting a neuroprotective effect. Statistical analysis. At least 600 randomly selected cells were counted in each experiment (n = 3, #P < 0.05 versus control, *P < 0.05 versus treated samples).

Dual staining (AO:EB): AO/EB dual staining was used to differentiate live, apoptotic, and necrotic cells. Live cells appeared green, early apoptotic cells showed green with condensed nuclei, while late apoptotic and necrotic cells appeared red/orange due to loss of membrane integrity. Rotenone-treated SH-SY5Y cells showed a significant increase in red/orange-stained cells compared to control, R+TPL, R+TPL-AgNPs, and R+LDA groups, confirming increased apoptosis [34] **figure 7.**

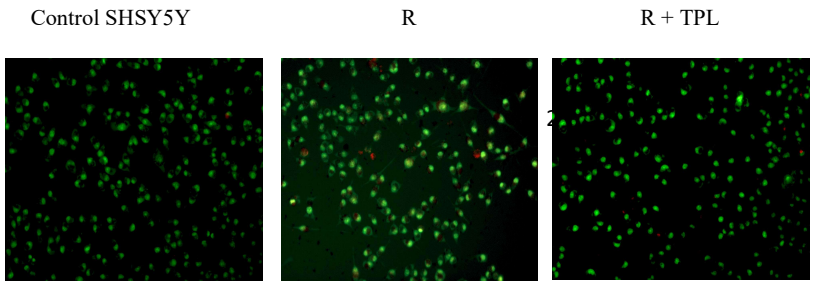

Figure: 7

Figure: 7 Illustrate the AO/EB dual staining was performed to assess cell viability and apoptosis in treated samples. Scale bar: 50 µm and representative fluorescence images show live (green), early apoptotic (yellow), and late apoptotic/necrotic (orange-red) cells under different conditions: Control, rotenone, R+TPL, R+TPL-AgNPs and R+LDA.

Expression of Bax, Bcl-2, caspase-3 and ERK-1: RT-qPCR analysis demonstrated that rotenone exposure significantly downregulated anti-apoptotic markers (Bcl-2 and ERK1) while upregulating pro-apoptotic markers (Bax and cleaved caspase-3) in SH-SY5Y cells. Conversely, treatment with TPL, TPL-AgNPs, and LDA restored the expression of Bcl-2 and ERK1 and suppressed Bax and caspase-3 levels, indicating a pronounced anti-apoptotic and cytoprotective effect shown in **figure 8** [35,36,37].

a

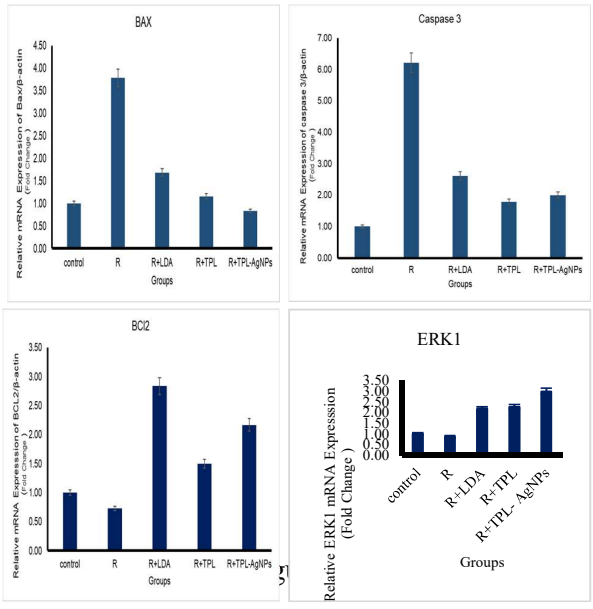

Figure 8: Illustrate the expression levels of Bcl-2 (anti-apoptotic), Bax (pro-apoptotic), Caspase-3 (apoptotic executioner) and ERK1 (phosphorylation) were analyzed in treated

samples. The protein expression across different treatment groups: Control, rotenone, R+TPL, R+TPL-AgNPs and R+LDA. Quantification of protein expression levels normalized to β-actin. Differentiated human SH-SY5Y cell line treated with rotenone significantly upregulated Bax and Caspase-3 expression while downregulating Bcl-2 and ERK1 indicating apoptotic cell death. Control, R+TPL, R+TPL-AgNPs and R+LDA reversed these effects, increasing Bcl-2 expression and ERK1 while reducing Bax and Caspase-3 levels, suggesting its neuroprotective role. Statistical analysis. At least 600 randomly selected cells were counted in each experiment ($n = 3$, #$P < 0.05$ versus control, *$P < 0.05$ versus treated samples).

Conclusion: Our results revealed that TPL-AgNPs might protect the differentiated SHSY5Y cells against OS induced by rotenone by modulating antioxidant status and apoptosis due to effective redox switching in nanoscale. Inhibition of ROS overproduction, preservation of mitochondrial function, modulation of anti- and pro-apoptotic proteins are related to the neuroprotective effects of TPL-AgNPs against rotenone induced apoptosis in dopaminergic SH-SY5Y cells.ss

Conflict of Interest:

There are no conflicts of Interest**References**:

1. Yamaguchi, S., Isaka, R., Sakahashi, Y., Tsujino, H., Haga, Y., Higashisaka, K., & Tsutsumi, Y. (2022). Silver nanoparticles suppress retinoic acid-induced neuronal differentiation in human-derived neuroblastoma SH-SY5Y cells. *ACS Applied Nano Materials, 5*(12), 19025–19034.
2. Scarpa, E., Cascione, M., Griego,A., Pellegrino, P., Moschetti, G., & De Matteis, V. (2023). Gold and silver nanoparticles in Alzheimer's and Parkinson's diagnostics and treatments. *iBrain, 9*(3), 298–315.
3. Beck, S., Mathison, H., Todorov, T., Calderón-Juárez, E. A., & Kopp, O. R. (2018). A review of medicinal uses and pharmacological activities of *Tridax procumbens* (L.). *Journal of Plant Studies, 7*(1), 19–35.
4. Thalkari, M. A. B., Karwa, M. P. N., Shinde, M. P. S., Gawli, C. S., & Chopane, P. S. (2020). Pharmacological actions of *Tridax procumbens* L.: A scientific review. *Research Journal of Pharmacognosy and Phytochemistry, 12*(1), 27–30.
5. Pringsheim, T., Day, G. S., Smith, D. B., Rae-Grant, A., Licking, N., Armstrong, M. J., et al. (2021). Dopaminergic therapy for motor symptoms in early Parkinson disease practice guideline summary: A report of the AAN guideline subcommittee. *Neurology, 97*(20), 942–957.
6. Hirsch, L., Jette, N., Frolkis, A., Steeves, T., & Pringsheim, T. (2016). The incidence of Parkinson's disease: A systematic review and meta-analysis. *Neuroepidemiology, 46*(4), 292–300.
7. Zeng, X. S., Geng, W. S., & Jia, J. J. (2018). Neurotoxin-induced animal models of Parkinson disease: Pathogenic mechanism and assessment. *ASN Neuro, 10*, 1759091418777438.
8. Javed, H., Amjad Kamal, M., & Ojha, S. (2016). An overview on the role of α-synuclein in experimental models of Parkinson's disease from pathogenesis to therapeutics. *CNS & Neurological Disorders - Drug Targets, 15*(10), 1240–1252.
9. Oertel, W., & Schulz, J. B. (2016). Current and experimental treatments of Parkinson disease: A

guide for neuroscientists. *Journal of Neurochemistry, 139*, 325–337.
10. Pakrashi, S., Chakraborty, J., & Bandyopadhyay, J. (2020). Neuroprotective role of quercetin on rotenone-induced toxicity in SH-SY5Y cell line through modulation of apoptotic and autophagic pathways. *Neurochemical Research, 45*(8), 1962–1973.
11. Li, Z., Xiao, G., Wang, H., He, S., & Zhu, Y. (2021). A preparation of *Ginkgo biloba* L. leaves extract inhibits the apoptosis of hippocampal neurons in post-stroke mice via regulating the expression of Bax/Bcl-2 and Caspase-3. *Journal of Ethnopharmacology, 280*, 114481.
12. Rajendran, G., Boopathy, U., Chandrasekar, S., & Durairaj, R. (2023). GC-MS and HPLC supported phytochemical analysis of *Tridax procumbens* Linn. leaves. *Journal of Advanced Zoology, 44*(6), 1770–1780.
13. Abbasi, E., Milani, M., Fekri Aval, S., Kouhi, M., Akbarzadeh, A., Tayefi Nasrabadi, H., et al. (2016). Silver nanoparticles: Synthesis methods, bio-applications and properties. *Critical Reviews in Microbiology, 42*(2), 173–180.
14. Karakuş, S., Baytemir, G., & Taşaltın, N. (2022). Digital colorimetric and non-enzymatic biosensor with nanoarchitectonics of *Lepidium meyenii*-silver nanoparticles and cotton fabric: Real-time monitoring of milk freshness. *Applied Physics A, 128*(5), 390.
15. Philip, D. (2010). Green synthesis of gold and silver nanoparticles using *Hibiscus rosa-sinensis*. *Physica E: Low-Dimensional Systems and Nanostructures, 42*(5), 1417–1424.
16. Rohini, D., & Vijayalakshmi, K. (2016). Sesamol antagonizes rotenone induced cell death in SH-SY5Y neuronal cells. *International Journal of Pharmacy and Pharmaceutical Sciences, 8*, 72–77.
17. Song, J., Hou, L., Ju, C., Zhang, J., Ge, Y., & Yue, W. (2013). Isatin inhibits proliferation and induces apoptosis of SH-SY5Y neuroblastoma cells *in vitro* and *in vivo*. *European Journal of Pharmacology, 702*(1–3), 235–241.
18. Kim, S., Min, S., Choi, Y. S., Jo, S. H., Jung, J. H., Han, K., et al. (2022). Tissue extracellular matrix hydrogels as alternatives to Matrigel for culturing gastrointestinal organoids. *Nature Communications, 13*(1), 1692.
19. Ramkumar, S. S., Sivakumar, N., Selvakumar, G., Selvankumar, T., Sudhakar, C., Ashokkumar, B., & Karthi, S. (2017). Green synthesized silver nanoparticles from *Garcinia imberti* Bourd and their impact on root canal pathogens and HepG2 cell lines. *RSC Advances, 7*(55), 34548–34555.
20. Nagabhishek, S. N., & Madankumar, A. (2019). A novel apoptosis-inducing metabolite isolated from marine sponge symbiont *Monascus* sp. NMK7 attenuates cell proliferation, migration and ROS stress-mediated apoptosis in breast cancer cells. *RSC Advances, 9*(11), 5878–5890.
21. Okamoto, A., Tanaka, M., Sumi, C., Oku, K., Kusunoki, M., Nishi, K., et al. (2016). The antioxidant N-acetyl cysteine suppresses lidocaine-induced intracellular reactive oxygen species production and cell death in neuronal SH-SY5Y cells. *BMC Anesthesiology, 16*(1), 104.
22. Zhang, Y., Su, S. S., Zhao, S., Yang, Z., Zhong, C. Q., Chen, X., et al. (2017). RIP1 autophosphorylation is promoted by mitochondrial ROS and is essential for RIP3 recruitment

into necrosome. *Nature Communications, 8*(1), 14329.
23. Niu, J., Li, C., Wu, H., Feng, X., Su, Q., Li, S., et al. (2015). Propidium iodide (PI) stains Nissl bodies and may serve as a quick marker for total neuronal cell count. *Acta Histochemica, 117*(2), 182–187.
24. Russo, R., Cassiano, M. G. V., Ciociaro, A., Adornetto, A., Varano, G. P., Chiappini, C., et al. (2014). Role of d-limonene in autophagy induced by bergamot essential oil in SH-SY5Y neuroblastoma cells. *PLoS One, 9*(11), e113682.
25. Liu, K., Liu, P. C., Liu, R., & Wu, X. (2015). Dual AO/EB staining to detect apoptosis in osteosarcoma cells compared with flow cytometry. *Medical Science Monitor Basic Research, 21*, 15.
26. Chomczynski, P., & Sacchi, N. (1987). Single-step method of RNA isolation by acid guanidinium thiocyanate-phenol-chloroform extraction. *Analytical Biochemistry, 162*(1), 156–159.
27. Sreelatha, S., Jeyachitra, A., & Padma, P. R. (2011). Antiproliferation and induction of apoptosis by *Moringa oleifera* leaf extract on human cancer cells. *Food and Chemical Toxicology, 49*(6), 1270–1275.
28. Ou, Z. Q., Rades, T., & McDowell, A. (2015). Anti-ageing effects of *Sonchus oleraceus* L. leaf extracts on H_2O_2-induced cell senescence. *Molecules, 20*(3), 4548–4564.
29. Singsai, K., Akaravichien, T., Kukongviriyapan, V., & Sattayasai, J. (2015). Protective effects of *Streblus asper* leaf extract on H_2O_2-induced ROS in SK-N-SH cells and MPTP-induced Parkinson's disease-like symptoms in C57BL/6 mouse. *Evidence-Based Complementary and Alternative Medicine, 2015*(1), 970354.
30. Kim, S., Park, S. E., Sapkota, K., Kim, M. K., & Kim, S. J. (2011). Leaf extract of *Rhus verniciflua* Stokes protects dopaminergic neuronal cells in a rotenone model of Parkinson's disease. *Journal of Pharmacy and Pharmacology, 63*(10), 1358–1367.
31. Elyasi, L., Jahanshahi, M., Jameie, S. B., Hamid Abadi, H. G., Nikmahzar, E., Khalili, M., & Jameie, M. (2021). 6-OHDA mediated neurotoxicity in SH-SY5Y cellular model of Parkinson disease suppressed by pretreatment with hesperidin through activating L-type calcium channels. *Journal of Basic and Clinical Physiology and Pharmacology, 32*(2), 11–17.
32. Kim, S., Kim, M., Kang, M. C., Lee, H. H. L., Cho, C. H., Choi, I., & Lee, S. H. (2021). Antioxidant effects of turmeric leaf extract against hydrogen peroxide-induced oxidative stress *in vitro* in Vero cells and *in vivo* in zebrafish. *Antioxidants, 10*(1), 112.
33. Gurunathan, S., Han, J. W., Eppakayala, V., Jeyaraj, M., & Kim, J. H. (2013). Cytotoxicity of biologically synthesized silver nanoparticles in MDA-MB-231 human breast cancer cells. *BioMed Research International, 2013*(1), 535796.
34. Olawale, F., Ariatti, M., & Singh, M. (2021). Biogenic synthesis of silver-core selenium-shell nanoparticles using *Ocimum tenuiflorum* L.: Response surface methodology-based optimization and biological activity. *Nanomaterials, 11*(10), 2516.
35. Liu, G., Wang, T., Wang, T., Song, J., & Zhou, Z. (2013). Effects of apoptosis-related proteins caspase-3, Bax and Bcl-2 on cerebral ischemia rats. *Biomedical Reports, 1*(6), 861–867.

36. Akhtar, R. S., Ness, J. M., & Roth, K. A. (2004). Bcl-2 family regulation of neuronal development and neurodegeneration. *Biochimica et Biophysica Acta (BBA) - Molecular Cell Research, 1644*(2–3), 189–203.
37. Song, J. X., Choi, M. Y. M., Wong, K. C. K., Chung, W. W. Y., Sze, S. C. W., Ng, T. B., & Zhang, K. Y. B. (2012). Baicalein antagonizes rotenone-induced apoptosis in dopaminergic SH-SY5Y cells related to Parkinsonism. *Chinese Medicine, 7*(1), 1.